J|A|C|S
ARTICLES
Published on Web 02/12/2003

Cross-Linked Normal Hexagonal and Bicontinuous Cubic Assemblies via Polymerizable Gemini Amphiphiles

Brad A. Pindzola,[†,‡] Jizhu Jin,[§] and Douglas L. Gin*[,§]

Contribution from the Department of Chemistry and Biochemistry, and Department of Chemical Engineering, University of Colorado, Boulder, Colorado 80309, and Department of Chemistry, University of California, Berkeley, California 94720

Received June 7, 2002; E-mail: gin@spot.colorado.edu

Abstract: The synthesis and lyotropic liquid-crystalline (LLC) phase behavior of a homologous series of intrinsically cross-linkable gemini surfactants are described. These novel bis(alkyl-1,3-diene)-based phosphonium gemini amphiphiles exhibit "normal" hexagonal (H_I), Type I bicontinuous cubic (Q_I), and lamellar (L_α) phases in water, and can be photocross-linked with retention of phase architecture in each case. On the basis of their locations on the phase diagram, their powder X-ray diffraction profiles, and the physical properties of the cross-linked materials, the Q_I phases formed by these gemini monomers are consistent with four possible bicontinuous cubic architectures with *P* or *I* space group symmetry that have been identified previously for small molecule amphiphiles. The extent of polymerization (i.e., the degree of diene conversion) achieved in the LLC phases was determined to be in the 23% to 71% range using UV−vis spectrometry, which is more than sufficient to extensively stabilize the systems. The resulting cross-linked H_I, L_α, and Q_I phases are stable up to 300 °C in air. To our knowledge, these reactive amphiphiles constitute the first example of a polymerizable gemini surfactant, and the first example of a cross-linkable amphiphile system that can be polymerized in both the H_I and a Q_I mesophase with retention of phase microstructure.

Introduction

Lyotropic liquid crystals (LLCs) are amphiphilic molecules that spontaneously organize in the presence of water into highly ordered yet fluid, phase-separated assemblies with periodic features on the 1−10 nm size regime.[1] Polymerizable versions of these molecules and their assemblies have recently generated a great deal of interest as a means of constructing functional nanostructured materials.[2] By polymerizing these ordered arrays of molecules into heavily cross-linked polymer networks, robust organic materials with unique nanoporous architectures can be generated that are ideal for the nanoscale reaction, encapsulation, and/or transport of molecules in either the aqueous or hydrocarbon domains.[2]

A large part of the interest in using reactive LLC assemblies for nanomaterials design stems from the fact that LLC phases offer exceptional control over nanoarchitecture because of the range of structures they form and the fact that the aqueous and hydrocarbon domains can adopt different relative locations with respect to each other (Figure 1).[1] LLC aggregate structures range from simple micelle systems to condensed anisotropic assemblies composed of ordered arrays of cylinders (i.e., hexagonal (H) phases), and bilayers (i.e., lamellar (L_α) phases). Depending on whether the hydrophobic/hydrophilic interface has a net positive mean curvature (i.e., curves toward the hydrophobic domains) or a net negative mean curvature (i.e., curves toward the aqueous domains),[1a] these phases can be further classified into Type I (oil-in-water, or "normal") or Type II (water-in-oil, or "inverted") phases. The L_α phase is considered to have zero mean curvature and serves as a midpoint in an idealized progression of LLC phases with increasing water content and curvature.[1] In addition to the L_α and H phases, a number of bicontinuous cubic (Q) phases have also been identified, which can exist between any of the LLC phases previously described and the simple micellar systems.[1,3] These Q phases are termed bicontinuous because they consist of two or more unconnected but interpenetrating hydrophobic and/or aqueous networks with overall cubic symmetry.[1,3,4] Depending on where they appear on the phase diagram relative to the central L_α phase, these Q phases can also be classified as Type I or Type II (i.e., they have the same cubic symmetries but inverted locations of the aqueous and hydrocarbon domains).[1a]

A number of reactive amphiphile systems have been designed that form L_α and H_{II} phases and retain their original LC phase

[†] Department of Chemistry, University of California, Berkeley.
[‡] Current address: ABS, Inc., 701-4 Cornell Business Park, Wilmington, Delaware 19801.
[§] Department of Chemistry & Biochemistry, and Department of Chemical Engineering, University of Colorado.

(1) For general reviews on LLC phases and their classifications, see: (a) Tate, M. W.; Eikenberry, E. F.; Turner, D. C.; Shyamsunder, E.; Gruner, S. M. *Chem. Phys. Lipids* **1991**, *57*, 147. (b) Seddon, J. M. *Biochim. Biophys. Acta* **1990**, *1031*, 1. (c) Tiddy, G. J. T. *Phys. Rep.* **1980**, *57*, 1.

(2) For reviews of nanostructured materials synthesis using polymerizable LLCs, see: (a) Gin, D. L.; Gu, W.; Pindzola, B. A.; Zhou, W.-J. *Acc. Chem. Res.* **2001**, *34*, 973. (b) Miller, S. A.; Ding, J. H.; Gin, D. L. *Curr. Opin. Colloid Interfac. Sci.* **1999**, *4*, 338. (c) O'Brien, D. F.; Armitage, B.; Benedicto, A.; Bennett, D. E.; Lamparski, H. G.; Lee, Y.-S.; Srisiri, W.; Sisson, T. M. *Acc. Chem. Res.* **1998**, *31*, 861. (d) Ringsdorf, H.; Schlarb, B.; Venzmer, J. *Angew. Chem., Int. Ed. Engl.* **1988**, *27*, 113.

(3) For reviews on bicontinuous cubic LLC phases, see: (a) Fontell, K. *Colloid Polym. Sci.* **1990**, *268*, 264. (b) Mariani, P.; Luzzati, V.; Delacroix, H. *J. Mol. Biol.* **1988**, *204*, 165.

(4) Benedicto, A. D.; O'Brien, D. F. *Macromolecules* **1997**, *30*, 3395.

10.1021/ja0208106 CCC: $25.00

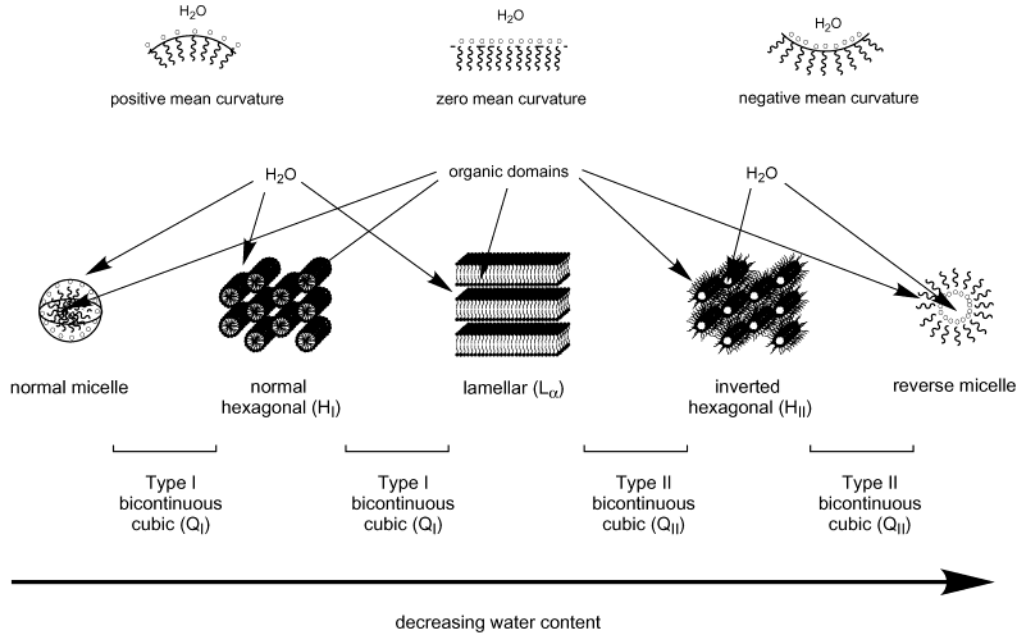

Figure 1. Schematic representation of an ideal progression of LLC phases as a function of system composition and mean curvature. The various bicontinuous cubic (Q) phases exist between the illustrated LLC phases and micellar structures.

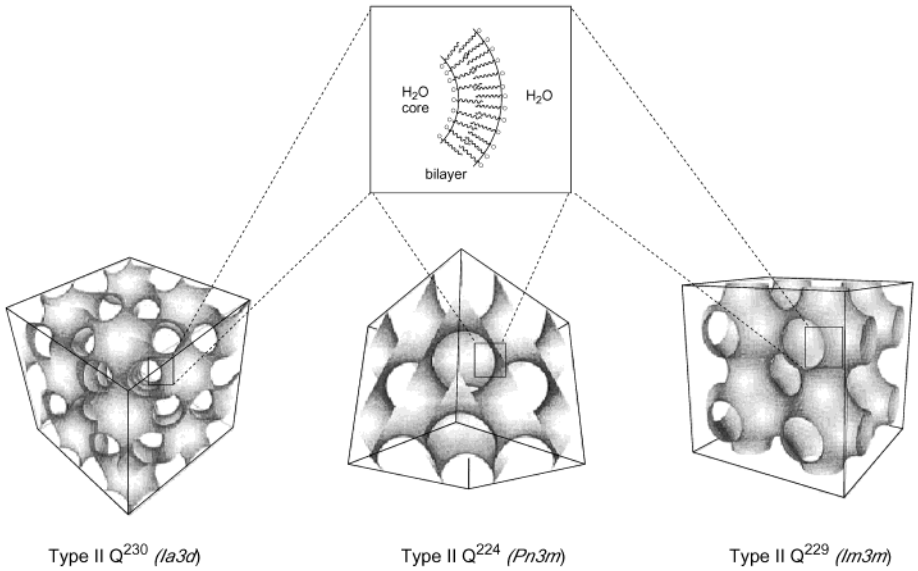

Figure 2. Schematic representations of three Q_{II} phases, showing the relative locations of the hydrocarbon (shaded regions) and aqueous domains (open white regions). The arrangement of the amphiphiles in these Q_{II} assemblies is illustrated in the inset. Partially reproduced from ref 4.

microstructure upon cross-linking.[2] These nanostructured materials have been successfully used in applications ranging from templated nanocomposite synthesis[5−9] to heterogeneous catalysis (i.e., organic molecular sieve analogues).[10,11] However, some LLC phases have remained more elusive with respect to in-phase polymerization and, thus, far less developed with respect to potential applications. Only four amphiphilic monomer systems have been reported that afford polymerized H_I assemblies.[12−15] These LLC monomers are all polymerizable single-tail surfactants, which require added cross-linkers to form robust networks, as opposed to soluble linear polysoaps. Even more rare are LLC systems that afford cross-linked Q phases with retention of phase structure. Early work by Anderson and Ström showed that replicas of Q_{II} networks with *Pn*3*m* symmetry (Type II Q^{224} (*Pn*3*m*)) (see Figure 2) can be formed via polymerization of conventional monomers (e.g., methyl methacrylate) in the organic regions of a Q_{II} phase formed by nonpolymerizable surfactants.[16] However, only one report of the successful cross-linking of reactive amphiphiles in a Q phase

(5) Smith, R. C.; Fischer, W. M.; Gin, D. L. *J. Am. Chem. Soc.* **1997**, *119*, 4092.
(6) Gray, D. H.; Hu, S.; Juang, E.; Gin. D. L. *Adv. Mater.* **1997**, *9*, 731.
(7) Gray, D. H.; Gin, D. L. *Chem. Mater.* **1998**, *10*, 1827.
(8) Sellinger, A.; Weiss, P. M.; Nguyen, A.; Lu, Y.; Assink, R. A.; Gong, W.; Brinker, C. J. *Nature* **1998**, *394*, 256
(9) Ding, J. H.; Gin, D. L. *Chem. Mater.* **2000**, *12*, 22.
(10) Miller, S. A.; Kim, E.; Gray, D. H.; Gin, D. L. *Angew. Chem., Int. Ed.* **1999**, *38*, 3021.
(11) Gu, W.; Zhou, W.-J.; Gin, D. L. *Chem. Mater.* **2001**, *13*, 1949.
(12) Herz, J.; Reiss-Husson, F.; Rempp, P.; Luzzati, V. *J. Polym. Sci., Part C* **1963**, *4*, 1275.
(13) Shibasaki, Y.; Fukuda, K. *Colloids Surf.* **1992**, *67*, 195.
(14) McGrath, K. M. *Colloid Polym. Sci.* **1996**, *274*, 399.
(15) Pindzola, B. A.; Hoag, B. P.; Gin, D. L. *J. Am. Chem. Soc.* **2001**, *123*, 4617.

has been published. O'Brien, Gruner, and co-workers showed that a mixture of two polymerizable dienoyl derivatives of naturally occurring phospholipids can be radically polymerized at elevated temperatures (60 °C) to afford a cross-linked Type II Q^{224} (*Pn*3*m*) phase.[17] Unfortunately, neither amphiphile by itself affords this Q_{II} phase, and the hydrated amphiphile mixture does not form the phase at ambient temperature.[17] More recently, O'Brien and co-workers designed a mixture of polymerizable lipids that form a Type II Q^{230} (*Ia*3*d*) phase (Figure 2); however, only soluble non-cross-linked polymers were formed by this system.[18]

There is a great deal of interest in designing new LLC monomer systems that efficiently form cross-linked H_I and Q phases because such stabilized assemblies offer new opportunities for applications as a result of their unique architectures. For example, cross-linking of the H_I phase would afford ordered arrays of polymer nanofibrils that could be useful as one-dimensional scaffolds for anisotropic nanocomposites, or as novel mineralization platforms[2a,15] in much the same way lipid microtubules have been employed.[19−21] Cross-linked Q assemblies have been proposed for applications ranging from membrane separations to bioencapsulation.[2a,c] Compared to H_{II} phases, cross-linked Q assemblies have even greater potential as nanoporous organic catalysts and membrane materials because they more closely mimic the interconnected channel structure of zeolites.[2a,c] Unlike the uniaxial H_{II} phase, Q materials would not require macroscopic alignment to facilitate substrate entry and transport because of their interconnected channel structures.[2a,c] Herein, we report a new family of intrinsically cross-linkable LLCs (**1**) based on gemini surfactants that provide convenient access to both cross-linked H_I and Q phases. These monomers are readily synthesized from nonbiological starting materials, and a number of homologues in this series exhibit H_I and Q_I phases under mild conditions in water (some even at ambient temperature). In addition, these monomers can be photocross-linked in both the H_I and Q_I phases with retention of phase microstructure, without the need for added cross-linkers or comonomers.

Results and Discussions

(a)LLC Monomer Design and Synthesis. For all practical purposes, the design of LLC monomers that adopt the H_I phase and ones that adopt the Q phases utilize two different sets of design considerations. The ability of a hydrated amphiphile system to preferentially form a particular LLC mesophase has been explained in two different ways: The first is a global approach which considers the interfacial energetics, tension, and intrinsic curvature of the amphiphile/water mixture as a collective ensemble.[1a,1b,22] The second approach examines the system on the microscopic level in terms of the molecular shape and packing preferences of the constituent amphiphiles (i.e., a surfactant packing parameter) to extrapolate the geometry of the preferred LLC phase.[23] Depending on the situation, one approach is sometimes better for rationalizing the behavior of certain LLC systems than the other. For example, changes in LLC phases with temperature and composition can be better rationalized by considering the interfacial energy and curvature of the entire system,[22] whereas the "shape" of the amphiphile apparently plays the more crucial role in determining mesophase geometry at fixed temperature and composition.[23] Amphiphiles that adopt the H_I phase have generally been rationalized by the shape-based approach, which is represented mathematically by the "critical packing parameter," $q = v/a_0 l_c$, where v is the effective hydrocarbon chain volume a_0 is the polar headgroup area; and l_c. is alkyl chain length of the surfactant.[23] According to this model, single-tailed amphiphiles with a "truncated cone" shape ($q \approx 0.5$) tend to pack into cylindrical micelles to form the H_I phase, whereas twin-tailed amphiphiles with an overall cylindrical shape ($q \approx 1$) tend to pack into L phases with no curvature, etc.[23] Thus, H_I monomers can be designed based on monomer shape and common structural elements. However, this shape-based approach appears to break down when it comes to understanding the Q phases which are considered curvature "saddle points".[1a] It turns out that a large number of single-tailed amphiphiles and two-tailed phospholipids ($q \approx 1$) with diverse structures can form Q phases, usually at elevated temperatures.[3a] Thus, the rational design of polymerizable amphiphiles that form Q phases based on similar structural motifs and packing principles is not very straightforward. The ability of amphiphiles to form Q phases is better rationalized in terms of balancing curvature and hydrocarbon chain stretching energies at the hydrophilic/hydrophobic interface;[1a,b] however, this approach makes molecular design difficult.

Recently, our research group designed a single-tailed LLC monomer, tetradeca-11,13-dienyl-trimethylphosphonium bromide (2), which can be photopolymerized in the H_I phase with and without added divinylbenzene (DVB) as cross-linker.[15] Compound 2 is a polymerizable phosphonium analogue of alkyltrimethylammonium bromide surfactants which have a "truncated cone" shape and are known to form the H_I phase as well as a Q_I phase with *Ia*3*d* symmetry.[24−26] Although this phosphonium diene monomer also forms a sizable cubic phase in water at temperatures above 35 °C; attempts to cross-link this Q phase proved to be very difficult and were only partially successful.[27] The reason for this difficulty was that the addition of DVB reduced the stable cubic phase regime to a very small region in the ternary phase diagram at ambient temperature.[28] To overcome these problems, an intrinsically cross-linkable derivative of tetradeca-11,13-dienyl-trimethylphosphonium bromide was desired that would provide assess to H_I and Q phases without the need for added comonomers.

The synthesis of an intrinsically cross-linkable monomer from a monofunctional monomer can simply be accomplished by the

(16) Anderson, D. M.; Ström, P. In *Polymer Association Structures. Microelmusions and Liquid Crystals*; El-Nokaly, M. A., Ed.; ACS Symposium Series 384; American Chemical Society: Washington, DC, 1989; Chapter 13.
(17) Lee, Y.-S.; Yang, J.-Z.; Sisson, T. M.; Frankel, D. A.; Gleeson, J. T.; Aksay, E.; Keller, S. L.; Gruner, S. M.; O'Brien, D. F. *J. Am. Chem. Soc.* **1995**, *117*, 5573.
(18) Srisiri, W.; Benedicto, A.; O'Brien D. F.; Trouard; T. P. *Langmuir* **1998**, *14*, 1921.
(19) Schnur, J. M.; Price, R.; Schoen, P.; Yager, P.; Calvert, J. M.; Georger, J.; Singh, A. *Thin Solid Films* **1987**, *152*, 181.
(20) Chappell, J. S.; Yager, P. *J. Mater. Sci. Lett.* **1992**, *11*, 633.
(21) Archibald, D. D.; Mann, S. *Nature*, **1993**, *364*, 430.
(22) (a) Gruner, S. M. *J. Chem. Phys.* **1989**, *93*, 7562. (b) Tate, M. W.; Gruner, S. M. *Biochemistry* **1989**, *28*, 4245.
(23) Israelachvili, J. N. *Intermolecular and Surface Forces with Applications to Colloidal and Biological Systems*; Academic: London, 1985; pp 249−257.
(24) Pindzola, B. A.; Gin, D. L. *Langmuir* **2000**, *16*, 6750.
(25) McGrath, K. M. *Langmuir* **1995**, *11*, 1835.
(26) Auvray, X.; Petipas, C.; Anthore, R.; Rico, I.; Lattes, A. *J. Phys. Chem.* **1989**, *93*, 7458.
(27) Pindzola, B. A., Ph.D. Thesis, University of California at Berkeley, 2001.
(28) See Supporting Information for ref 15.

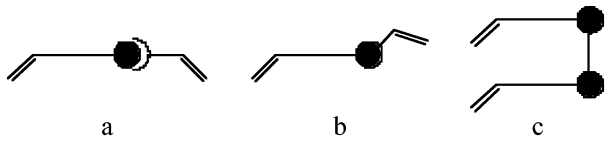

Figure 3. Schematic representations of three general approaches to making an intrinsically cross-linkable LLC monomer from a monofunctional LLC monomer.

addition of a second chain-addition polymerizable moiety to the molecule. In our case, this is complicated by the need to maintain an appropriate molecular geometry for the desired LLC phase behavior.[23] Consequently, a second polymerizable tail cannot be simply attached to the amphiphile because this modification would drastically change the overall molecular shape. Figure 3 shows several alternative approaches for creating a cross-linkable analogue of **2** that should retain the desired LLC architecture on polymerization. The first approach (Figure 3a) is to employ a polymerizable counterion such as a (meth)-acrylate or 4-vinylbenzoate, following the work of Ringsdorf[29] and Kline.[30] This method has the benefit of being a relatively simple and minor modification to the existing amphiphile; however, that the connection between the polymerizable groups in each monomer would no longer be a covalent bond but rather a weaker, ionic interaction. This approach is currently being explored in our group.[31] A second approach (Figure 3b) is to append a polymerizable moiety to the headgroup. This route would maintain the covalent connection between the polymerizable groups, but it would also be very synthetically challenging and may detrimentally alter the overall molecular shape. The final potential solution to this problem (Figure 3c) is to make a polymerizable dimeric or "gemini" version of **2**. The term "gemini surfactant" was originally coined by Menger to describe a relatively new class of amphiphiles composed of two classical single-tail amphiphiles connected covalently at the headgroup by a spacer.[32] Gemini surfactants of the general structure CH_3-$(CH_2)_n N^+(CH_3)_2(CH_2)_m N^+(CH_3)_2(CH_2)_n CH_3$, with a flexible spacer of moderate length ($m = 6-10$), have demonstrated LLC behavior similar to that of the monomeric amphiphiles of the same tail length (e.g., spherical micelles, cylindrical micelles, L_α phases, and vesicles).[33] By synthesizing a dimeric version of our single-tail phosphonium monomer, it was hoped that an intrinsically cross-linkable LLC exhibiting H_I and Q phases would be accessible. To our knowledge, polymerizable gemini amphiphiles are unprecedented, and their LLC and polymerization behavior are completely unknown.

The general synthesis of gemini surfactants (**1a**−**i**) based on polymerizable dienyltrimethylphosphonium bromide salts is depicted in Scheme 1. 1,2-bis(Dimethylphosphino)ethane is a commercially available reagent, but the other two bis(dimethylphosphino)alkanes had to be prepared from the reaction of two equivalents of sodium dimethylphosphide (generated in situ from sodium and tetramethyldiphosphine) with either 1,6-dibromohexane or 1,8-dibromooctane in an adaptation of a procedure developed by Kordosky.[34] Reaction of the bis-

Scheme 1

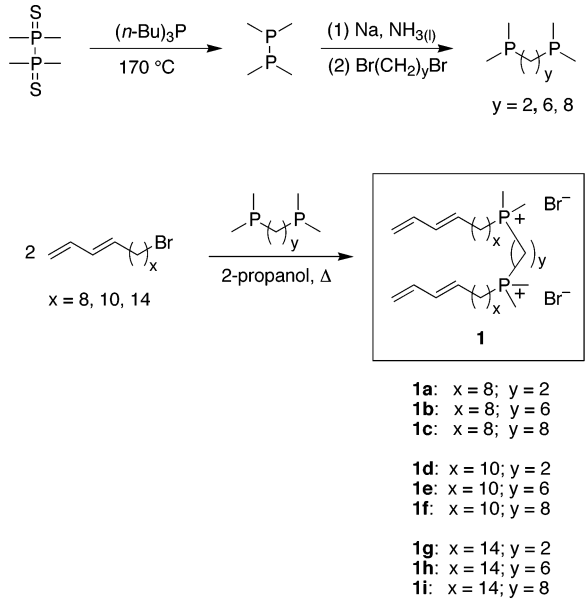

1a: x = 8; y = 2
1b: x = 8; y = 6
1c: x = 8; y = 8

1d: x = 10; y = 2
1e: x = 10; y = 6
1f: x = 10; y = 8

1g: x = 14; y = 2
1h: x = 14; y = 6
1i: x = 14; y = 8

(dimethylphosphino)alkanes with two equivalents of ω-bromoalkyl-1,3-diene[15] in 2-propanol at elevated temperature gave the desired products, which were recrystallized from ethyl acetate. A series of nine homologues of **1** with three different tail lengths ($x = 8$, 10, and 14) and three different headgroup spacer lengths ($y = 2$, 6, and 8) were synthesized in order to examine the effect of these two parameters on LLC behavior and in-phase polymerization. It should be noted that these polymerizable gemini surfactants are not stable in air at room temperature for extended periods of time, so they were stored at 0 °C under a nitrogen atmosphere.

(b)LLC Phase Behavior and Characterization. Once the polymerizable gemini amphiphiles were synthesized, their two-component phase diagrams with water were mapped out using polarized light microscopy (PLM) as a function of temperature. The identities of the observed LLC phases in each case were assigned as follows, based on their PLM optical textures, low-angle powder X-ray diffraction (XRD) patterns, and relative positions on the phase diagram: The L_α phase, which is generally considered the midpoint of an ideal LLC phase progression, is identified by a bright mosaic-type optical texture and an XRD profile in which the observed *d* spacings proceed in the ratio 1:1/2:1/3:1/4..., (i.e., the d_{100}, d_{200}, d_{300}, d_{400},... diffraction planes).[1] The H phases exhibit a bright striated optical texture, and their XRD profiles exhibit a *d* spacing pattern that proceeds in the ratio: $1:1/\sqrt{3}:1/\sqrt{4}:1/\sqrt{7}$... (i.e., d_{100}, d_{110}, d_{200}, d_{210},...).[1] An H phase appearing on the water-rich side of the L_α phase on the phase diagram is generally assumed to be an H_I phase. Conversely, an H phase that appears on the water-poor side of the L_α phase is regarded as an H_{II} phase.[1a,b] In the absence of observable secondary or higher order XRD reflections, L_α and H phases can be distinguished via their optical textures and their location on the phase diagram with respect to other phases (see Figure 1).[1] In contrast, Q phases are all optically isotropic by PLM but exhibit an XRD pattern with symmetry-allowed *d* spacings that ideally proceed in the ratio: $1:1/\sqrt{2}:1/\sqrt{3}:1/\sqrt{4}:1/\sqrt{5}:1/\sqrt{6}:1/\sqrt{8}:1/\sqrt{9}:1/\sqrt{10}$... (cor-

(29) (a) Ringsdorf, H.; Schlarb, B.; Tyminski, P. N.; O'Brien, D. F. *Macromolecules* **1988**, *21*, 671. (b) Ringsdorf, H.; Schlarb, B. *Makromol. Chem.* **1988**, *189*, 299.
(30) Kline, S. R. *Langmuir* **1999**, *15*, 2726.
(31) Markevitch, D. M.; Pindzola, B. A.; Gin, D. L. *Polym. Prepr., Am. Chem. Soc. Div. Polym. Chem.* **2001**, *42*(1), 537.
(32) Menger, F. M.; Littau, C. A. *J. Am. Chem. Soc.* **1991**, *113*, 1451.
(33) Buhler, E.; Mendes, E.; Boltenhagen, P.; Munch, J. P.; Zana, R.; Candau, S. J. *Langmuir* **1997**, *13*, 3096.
(34) Kordosky, G.; Cook, B. R.; Cloyd, J. J.; Meek, D. W. *Inorg. Synth.* **1973**, *14*, 14.

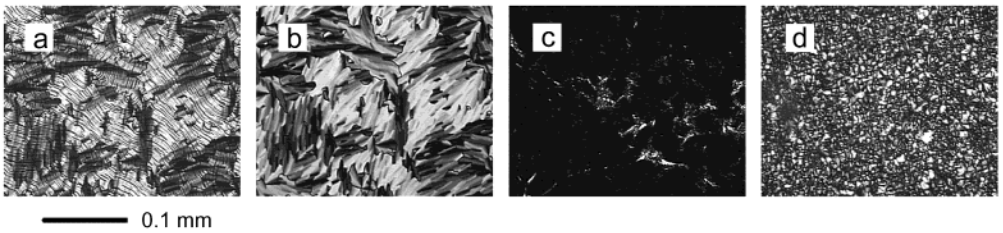

Figure 4. Representative PLM optical textures of the LLC phases of the cross-linkable gemini surfactants: (a) an unidentified LLC phase (**1e** at 39 wt % in water, 24 °C); (b) the H_I phase (**1e** at 39 wt % in water, 50 °C); (c) the Q_I phase (**1i** at 85 wt % in water, 24 °C); and (d) the L_α phase (**1e** at 90 wt % in water, 95 °C). All images were taken at 12.6 X magnification.

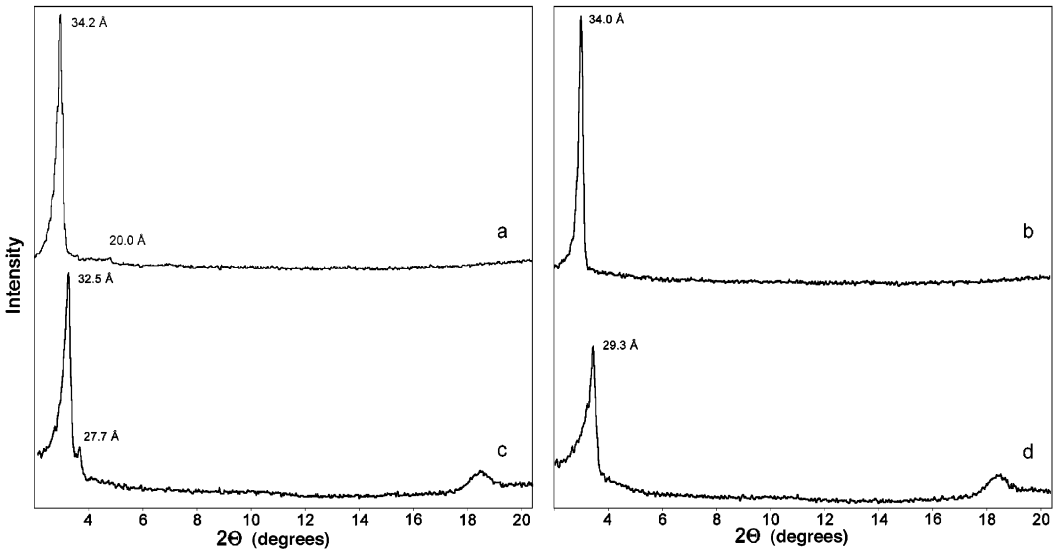

Figure 5. Representative XRD patterns for the LLC phases observed in the cross-linkable gemini surfactants: (a) Unidentified LLC phase (**1e**, 64 wt % in water, 24 °C); (b) H_I phase (**1e**, 75 wt % in water, 24 °C); (c) Q_I phase (**1e**, 85 wt % in water, 35 °C); and (d) L_α phase (**1e**, 90 wt % in water, 62 °C). The broad peak just above 18° in 2θ in (c) and (d) results from the Mylar windows on the programmable XRD capillary oven.

responding to the d_{100}, d_{110}, d_{111}, d_{200}, d_{210}, d_{211}, d_{220}, d_{221} (or d_{300}), d_{310},... diffraction planes).[1,3] It should be noted that there are a number of different Q phase architectures possible,[3b,35] and that systematic XRD absences in the XRD peaks result as the cubic unit cell becomes more complex. The three-dimensional structures of many Q phases have been elucidated from detailed electron microscopy and two-dimensional XRD studies.[3,35−40] For convenience, the presence of Q phases with *P* or *I* symmetry in polydomain small molecule amphiphile[3] and phase-separated block copolymer systems[35−40] has generally been identified on the basis of a black optical texture and a powder XRD profile in which the $1/\sqrt{6}$ and $1/\sqrt{8}$... d spacings (i.e., the d_{211} and d_{220} reflections) are at least present.[17,35] To unequivocally distinguish between the various 3-D cubic phase architectures, however,[3b] a sufficient number of higher order XRD reflections must be observable.[3b,35,36] As in the case of the H phases, Q phases that appear on the water-rich side of the L_α phase of the phase diagram are considered Q_I phases, and those that appear on the water-poor side are regarded as Q_{II} phases.[1a,b] Representative optical textures and XRD profiles for each observed LLC phase for the homologues of **1** are shown in Figures 4 and 5, respectively.

Using these systematic phase identification guidelines, it was found that the three gemini monomers with the shortest tails (**1a**−**c**, $x = 8$) exhibit relatively simple phase behavior. The phase diagram for **1a** ($y = 8$, $x = 2$) (Figure 6a) shows only a relatively small H_I phase region that extends from 67 to 85 wt % amphiphile at temperatures of up to 55 °C. Similarly, the phase diagram for **1b** ($x = 8$, $y = 6$) (Figure 6b) only shows an H_I regime that extends from 68 to 85 wt % amphiphile and up to a maximum temperature of 58 °C. Compound **1c** ($x = 8$, $y = 8$) in contrast does not display any LLC behavior at all: it only exhibits a fluid isotropic phase (I) below 95 wt % amphiphile.

The polymerizable gemini surfactants with the midrange tail length (**1d**−**f**, $x = 10$) have a more complex phase behavior in general. The phase diagram for **1d** ($x = 10$, $y = 2$) exhibits two distinct LLC phases (Figure 6c). At lower percentages of amphiphile (55−80 wt %) and slightly elevated temperature (30−75 °C), a rather broad Q phase is observed. Moving to higher concentration of amphiphile (80−90 wt %) and higher temperatures (55 to >100 °C), an L_α phase is observed. Because this Q phase appears on the water-rich side of the phase diagram with respect to the L_α phase, it should be classified as a Q_I phase with net positive mean curvature. The phase diagram for **1e** ($x = 10$, $y = 6$) (Figure 6d) exhibits four different LLC phases. An H_I phase extends from 48 to 81 wt % amphiphile at ambient temperature to more than 100 °C, depending on

(35) Hajduk, D. A.; Harper, P. E.; Gruner, S. M.; Honeker, C. C.; Kim, G.; Thomas, E. L.; Fetters, L. J. *Macromolecules* **1994**, *27*, 4063.
(36) Hajduk, D. A.; Harper, P. E.; Gruner, S. M.; Honeker, C. C.; Kim, G.; Thomas, E. L.; Fetters, L. J. *Macromolecules* **1995**, *28*, 2570.
(37) Sakurai, S. *Trends Polym. Sci.* **1997**, *5*, 210.
(38) Lipic, P. M.; Bates, F. S.; Hillmyer, M. A. *J. Am. Chem. Soc.* **1998**, *120*, 8963.
(39) Lee, M.; Cho, B.-K.; Kim, H.; Yoon, J.-Y.; Zin, W.-C. *J. Am. Chem. Soc.* **1998**, *120*, 9168.
(40) Shefelbine, T. A.; Vigild, M. E.; Matsen, M. W.; Hajduk, D. A.; Hillmyer, M. A.; Cussler, E. L.; Bates, F. S. *J. Am. Chem. Soc.* **1999**, *121*, 8457.

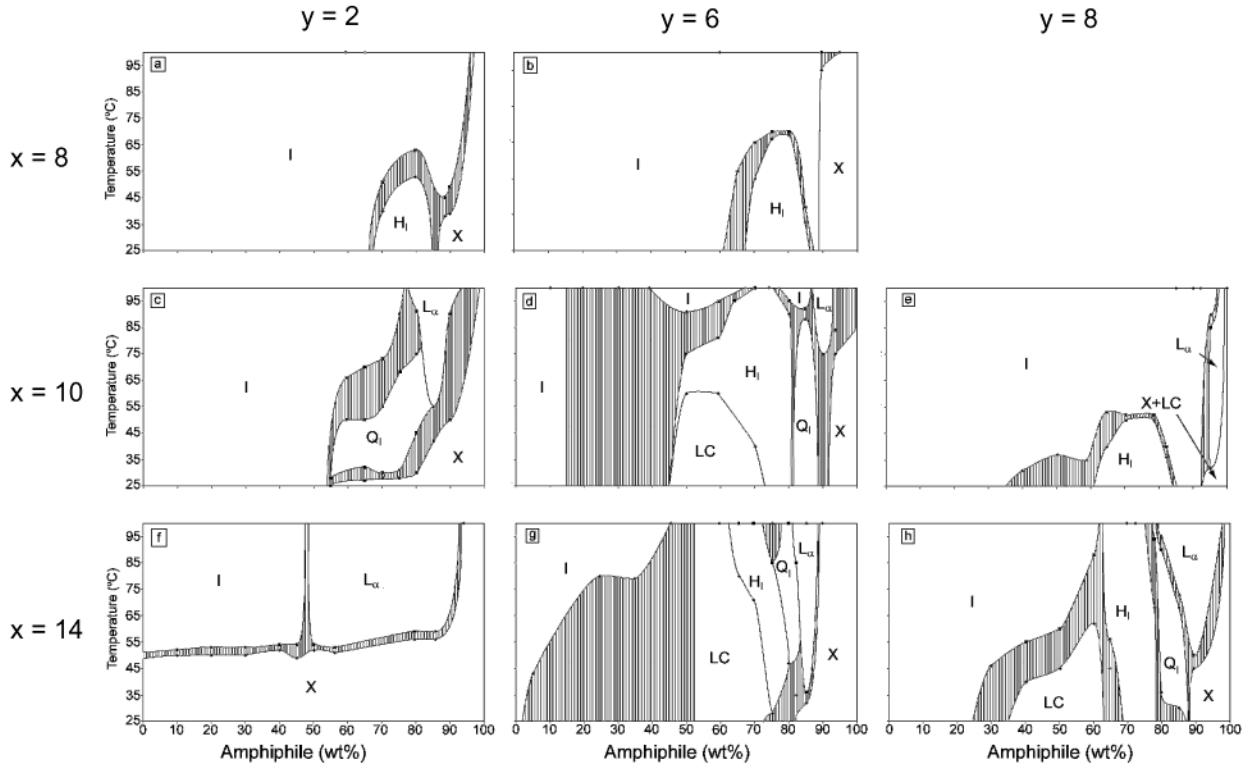

Figure 6. Phase diagrams for the eight polymerizable gemini surfactants that displayed LLC behavior in water: (a) compound **1a**, (b) compound **1b**, (c) compound **1d**, (d) compound **1e**, (e) compound **1f**, (g) compound **1h**, and (h) compound **1i**. The phase diagram for compound **1c** is not included because **1c** did not display any LLC behavior. (LC = unidentified LLC phase; I = fluid isotropic phase; X = crystalline phase. Vertical hashing indicates areas where two or more phases coexist.) These phase diagrams were mapped out at U. C. Berkeley (near sea level, >50% relative humidity. They will be slightly different at higher altitudes.

amphiphile concentration. A narrow Q_I phase region extends from 82 to 88 wt % amphiphile at 25 °C to 87 °C. This Q_I phase is followed by an L_α phase that extends from 87 to 93 wt % amphiphile at temperatures of 75 °C and above. Finally, an as yet unidentified LC phase exists from 45 to 73 wt % amphiphile at ambient temperature up to a maximum of 60 °C. From the PLM micrographs, it can be seen that the optical texture for this unidentified LLC phase (Figure 4a) is similar to that observed for the H_I phase surrounding it on the higher concentration amphiphile side. However, the phase in question has distinct and reversible differences which do not correspond to any of the generally accepted LLC phases. Unfortunately, powder XRD was not useful in identifying this phase because it only exhibits a single, strong reflection. One of two possibilities for this mesophase seem most likely. It could be one of the so-called "intermediate" phases,[41,42] or simply a mixtures of phases. "Intermediate" LLC phases generally appear between the H and L_α phases, frequently in place of Q phases.[41,42] These optically anisotropic phases are proposed to have rectangular, layered, rhombohedral, and tetragonal symmetries; and are believed to have ribbon or mesh-like structures. The fact that the unidentified LLC phase appears between the fluid isotropic (I) phase and the H_I phase, rather than between the H_I and L_α phases, argues against it being one of the other better known intermediate phases. It seems most likely that it is simply a mixture of phases, but an uncommon intermediate phase cannot be ruled out from the data available. Finally, compound **1f** ($x = 10$, $y = 8$) (Figure 6e) exhibits two LLC phases: an H_I domain and an L_α domain. The H_I phase of **1f** spans 61 to 83 wt % amphiphile and exists up to 51 °C. The L_α region extends from 95 to 98 wt % amphiphile and exists above 33 °C.

The three members in the homologous series with the longest tails (**1g**−**i**, $x = 14$) also display rich and diverse LLC phase behavior. The phase diagram for compound **1g** ($x = 14$, $y = 2$) (Figure 6f) is the simplest of the three, displaying only an L_α phase from 49 to 93 wt % amphiphile and above ca. 55 °C. Interestingly, this homologue is the only compound in the entire nine compound series which has a Krafft point (i.e., an order−disorder transition temperature for the alkyl chains) above room temperature across the entire range of concentrations studied. Presumably, the long alkyl tails and the close proximity of the tethered headgroups (due to the short spacer length) favor more ordered hydrocarbon tail packing than in the other molecules. In contrast, compound **1h** ($x = 14$, $y = 6$) (Figure 6g) displays four different LLC phases: the same unidentified LLC phase as in **1e**, plus an H_I, a Q_I, and an L_α phase. The unidentified mesophase extends from 52 to 74 wt % amphiphile and from less than 25 °C to greater than 100 °C in temperature. From 74 to 78 wt % amphiphile and from 27 °C to greater than 100 °C, the H_I phase is observed. Following the H_I phase and extending to 83 wt % amphiphile from 46 °C to greater than 100 °C is a Q_I phase. Finally, an L_α phase exists from 83 to 88 wt % amphiphile above 36 °C. Compound **1i** ($x = 14$, $y = 8$) (Figure 6h) displays the same four LLC phases seen in the previous case. The unidentified LLC phase exists between 35 and 64 wt % amphiphile and from below ambient temperature to a maximum temperature of 62 °C. The H_I phase extends from 66 to 78 wt % amphiphile and from less than 25 °C to greater

(41) Luzzati, V.; Mustacchi, H.; Skoulios, A.; Husson, F. *Acta Crystallogr.* **1960**, *13*, 660.
(42) Hagslatt, H.; Soderman, O.; Jonsson, B. *Liq. Cryst.* **1994**, *17*, 157.

than 100 °C. The Q_I phase exists from 80 to 88 wt % amphiphile and from about 30 °C to 90 °C. The L_α phase exists at higher temperatures and on the water-poor side of the Q_I phase, extending from 80 to 98 wt % amphiphile and above 50 °C.

Certain trends in LLC phase behavior for the gemini homologues can also be observed by considering the headgroup spacer length (y) instead of the hydrocarbon tail length (x). It is known that the LLC properties of gemini surfactants are highly dependent on the length of the flexible spacer between the polar headgroups.[33] The reason for this strong dependence is based on shape-based principles and packing parameter:[33] The headgroup area of a gemini surfactant (a_o) has been found to increase in a nonmonotonic manner with spacer length. It increases rapidly for short spacers (<10 methylene units), reaches a maximum for medium spacers (10−12 methylene units), and then decreases for longer spacers (≥14 methylene units).[33] A closer examination of the phase diagrams of **1a**−**i** presented in Figure 6 shows that the polymerizable gemini surfactants exhibit the same sensitivity to headgroup spacer length. On going across each row of phase diagrams, the number and size of stable LLC domains exhibited by gemini monomers with the same tail length (x) generally increases as y goes from 2 to 6, but then decreases when y reaches 8. These gemini monomers are in the "short" spacer regime (<10 methylenes), so these changes reflect the fact that a_o increases rapidly with increasing spacer length. However, it is important to observe the interplay between spacer length and tail length in determining the overall ability of these gemini systems to form certain LLC phases. At short tail lengths ($x = 8$), the gemini monomers can only form the H_I phase with varying spacer length, indicating that a_o is sufficiently large in the $y = 2-8$ range that the surfactants cannot adopt the general cylindrical shape ($q \approx 1$) needed to form bilayer type L (and Q) phases. In fact, as y reaches 8 for this tail length, it appears that a_o is so large that even the truncated conical shape needed to form H_I phases is disrupted, and no LLC phases are observed. However, as the tail length increases ($x = 10$ and 14) (and presumably so does the effective hydrocarbon tail volume), the resulting longer gemini surfactants are better able to adopt an overall cylindrical shape to form L and Q phases, even with increasing spacer length. As can be seen in Figure 6, the gemini homologues that are best able to form L and Q type phases are the ones with "matched" spacer and tail lengths (i.e., medium spacer with medium length tails, or longer spacer with longer tails). Qualitatively at least, it appears that for these gemini surfactants, certain aspects of the shaped-based LLC model apply. That is, increases in a_o via spacer effects can be offset by increasing tail length and hydrocarbon chain volume so that certain shapes and values of the packing parameter q can be maintained.

Unfortunately, only two powder XRD peaks ($1/\sqrt{6}$, $1/\sqrt{8}$) were generally observed for the observed Q_I phases of the **1** homologues, indicating that they do not possess a great deal of long range order. In an attempt to obtain more data on the architecture of the Q_I phases, the samples were also analyzed by two-dimensional X-ray scattering with a higher intensity X-ray source. Unfortunately, the Q_I samples were all polydomain in nature and could not be easily aligned resulting in diffraction rings rather than spots in the 2-D XRD images (see Supporting Information). In addition, higher order reflections were not observed under these conditions. Attempts were also made to image the Q_I structures of **1e** by transmission electron microscopy (TEM), and atomic force microscopy (AFM). Unfortunately, the TEM images obtained with extensively stained and embedded samples were of insufficient resolution to conclusively show a cubic structure,[43,44] and the sample surfaces were too rough to obtain high-resolution AFM images (see Supporting Information). Consequently, it was not possible to unambiguously identify which of the possible cubic architectures[3b] the observed Type I Q phases might be. However, based on their one-dimensional XRD profiles, their locations on the phase diagrams, and the physical properties of the cross-linked materials, it was possible to narrow down the possibilities.

According to Luzzati and co-workers, six geometrically distinct Q phase architectures have been identified so far in small molecule amphiphile systems, based on their detailed XRD data, symmetry, and common structural elements (i.e., Q^{230} (*Ia*3*d*), Q^{224} (*Pn*3*m*), Q^{229} (*Im*3*m*), Q^{212} ($P4_32$), Q^{227} (*Fd*3*m*), and Q^{223} (*Pm*3*n*); see Supporting Information).[3b] It turns out that cubic mesophases consisting entirely of closed normal or reverse micelles are quite rare, and their structures have not been substantiated.[1a,3a] Of the six Q phase architectures so far identified in amphiphile systems,[3b] the combined data obtained for the gemini Q_I phases are consistent with a Q^{230} (*Ia*3*d*), Q^{224} (*Pn*3*m*), Q^{229} (*Im*3*m*), or Q^{212} ($P4_32$) phase of Type I configuration. The fact that $1/\sqrt{6}$ and $1/\sqrt{8}$ peaks are exhibited by all the Q_I phases of the gemini monomers indicates that they cannot have the Q^{227} (*Fd*3*m*) architecture. The Q^{227} (*Fd*3*m*) phase has *F* symmetry and does not have a symmetry-allowed $1/\sqrt{6}$ (i.e., d_{211}) reflection.[3b,35] The Q^{223} (*Pm*3*n*) phase can also be ruled out with a high degree of confidence, based on our polymerization results described in the proceeding section. A Type I Q^{223} (*Pm*3*n*) phase is believed to be either a system composed entirely of closed micelles with the hydrophobic tails located in the micelle interiors, or at most a system composed of independent micelles and a single channel network (see the Supporting Information).[3b] If this system were to be polymerized at the tail ends, there would be minimal inter-micelle connectivity and perhaps only a single polymerized channel system, resulting in a polymer with very poor mechanical and thermal integrity. As described in the polymerization results section, all of the cross-linked Q_I phases of the gemini monomers exhibit excellent mechanical integrity and thermal stability. Thus, the Q_I phases of the gemini monomers can be inferred to be one of the remaining four Q architectures with *P* or *I* symmetry which have a more extensive interpenetrating channel system. A Type I Q^{230} (*Ia*3*d*) phase appears to be the most likely candidate for two reasons: First, Q phases with *Ia*3*d* symmetry are the most common Q phases observed between the L_α and H phases.[3a] Second, the monomeric alkyltrimethylammonium salts from which the gemini amphiphiles are derived exhibit a Q phase with *Ia*3*d* symmetry on the water-rich side of the L_α phase.[24,25] Regardless of which may be the actual case, the four possible Q_I phases for the polymerizable gemini surfactants are all bicontinuous, with aqueous and organic networks that permeate the sample in three dimensions. They would still make intriguing candidates for nanoporous organic transport and catalysis media if they can be stabilized by cross-linking.

(43) Because of the poor quality of the TEM images, electron diffraction studies were not performed on the gemini Q_I phases.
(44) To our knowledge, successful STM and AFM imaging of cross-linked LLC phases has not reported.

(c)In Situ Cross-Linking of the LLC Phases. Once the general LLC phase behavior of the polymerizable gemini surfactants was characterized, their polymerization behavior in the various LLC phases was subsequently examined. Three issues with respect to the in-phase polymerization of these monomers were investigated. The first issue was whether these reactive gemini LLCs can be cross-linked without significant disruption of the phase structures. This was determined by comparing the PLM optical textures and XRD patterns of the samples before and after radical photopolymerization. The second issue was determining the degree of polymerization (or at least the extent of 1,3-diene conversion) in these systems. Typically the degree of polymerization in cross-linkable 1,3-diene-based LC monomers can be estimated using FT-IR spectroscopy by monitoring the decrease in intensity of the C=C stretching bands at 1602 and 1651 cm^{-1}.[15,45] In the case of LLC systems, D_2O must be used in place of H_2O to eliminate the strong overlapping H−O−H band at 1600 cm^{-1}.[15] Unfortunately, FT-IR spectroscopy could not be employed because the baselines in the FT-IR spectra of the gemini LLC mixtures did not remain level or consistent. The degree of 1,3-diene polymerization was estimated instead using UV−vis spectroscopy, because polymerization of a 1,3-diene moiety leads to loss of conjugation.[46] The degree of conversion can be determined by comparing the intensity of the 1,3-diene absorption band (λ_{max} = 226 nm) in the samples before and after irradiation, similar to protocols used to study the polymerization of the related sorbate moiety in amphiphile/water mixtures.[46] With very thin films of the room-temperature LLC phases on quartz or CaF_2 plates, it was possible to obtain reproducible UV−vis spectra of the monomers and polymers in those phases.[47] The third issue was the stability and robustness of the cross-linked LLC phases. This was assessed by heating the LLC networks in air and observing the temperature at which the LLC order was disrupted as indicated by changes in the PLM optical textures.

It was found that the LLC mixtures of the gemini monomers can be photopolymerized by 365 nm light either with 1−2 wt % 2,2-dimethoxyphenylacetophenone as a radical photoinitiator, or without any added photoinitiator at all. No appreciable difference was observed in the extent of conversion achieved between samples that included 2,2-dimethoxyphenylacetophenone and those that did not. Thus, all photopolymerization studies were performed without added photoinitiator for simplicity of sample preparation.

As described in the previous section, six of the nine homologues of **1** display an H_I phase. In all six cases, radical photopolymerization of the monomers in the H_I phase proceeded with retention of the phase architecture, as seen by PLM and XRD. A representative view of polymerization of monomers in the H_I phase is shown in Figure 7. A summary of the positions of the primary d_{100} XRD peak before and after irradiation, the thermal stability of the phase after irradiation and the extent of conversion for the six molecules polymerized in the H_I phase are presented in Table 1.

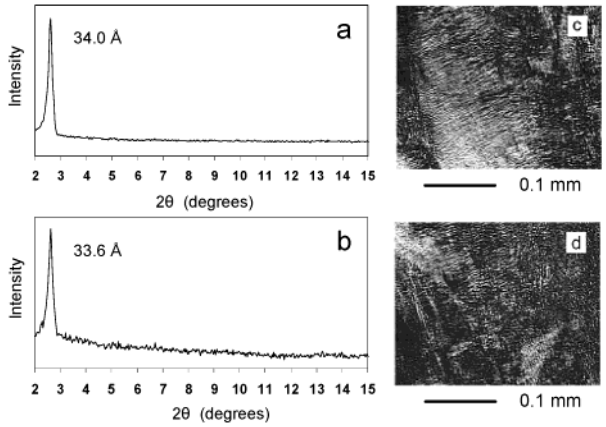

Figure 7. Representative XRD profiles and PLM optical textures of the H_I phases of the gemini monomers before and after photopolymerization: (a) XRD pattern of **1e** (75 wt % in water, 24 °C) before photopolymerization; (b) XRD pattern of **1e** (75 wt % in water, 24 °C) after photopolymerization; (c) PLM micrograph of **1e** (75 wt % in water, 24 °C) before photopolymerization; and (d) PLM micrograph of **1e** (75 wt % in water, 24 °C) after photopolymerization.

Table 1. Summary of Data for Molecules Polymerized in the H_I Phase[a]

compd	d_{100} before irradiation (Å)	d_{100} after irradiation (Å)	polymerized phase thermal stability (°C)	extent of conversion (%)
1a	31.3	31.0	> 300	60
1b	29.8	29.4	> 300	71
1e	34.0	33.6	> 300	40
1f	35.9	33.1	> 300	44
1h	42.5	41.4	> 300	N/A
1i	41.7	42.3	> 300	23

[a] Extent of conversion via UV−vis is unavailable for compound **1h** in the H_I phase because that phase does not exist at room temperature.

From the PLM micrographs in Figure 7, it is obvious that the H_I phase is being maintained upon polymerization since there is little change in the optical textures before and after irradiation. After polymerization, variable temperature PLM showed that the H_I phase is stable up to at least 300 °C, above which severe degradation of the material itself begins. In contrast, the unpolymerized phases either clear below, or begin to rapidly lose water around 100 °C. As can be seen in Figure 7 and Table 1, XRD shows that there is slight disordering of the phases upon cross-linking based on the loss in peak intensity observed in all cases. However, the overall symmetry of the phase is retained. Additionally, the dimensions of the H_I phases slightly decrease (at most by 3 Å) upon polymerization in almost every case, as would be expected upon cross-linking.[48] Finally, a general decrease is seen in the extent of conversion with increasing tail length. Unfortunately, not enough data is available to see any trends with regard to the length of the spacer between the two headgroups. Extents of polymerization in the H_I phases vary from 23 to 71% diene conversion by UV−vis spectroscopy. However, even with the lowest observed extent of conversion observed in our H_I assemblies (23%), an extensively stabilized cross-linked structure is still achieved. The gel point for chain addition polymerization, ρ_c, is given by the equation: $\rho_c = ([A] + [B])/([B]X_w)$, where [*A*] is the concentration of monofunc-

(45) Hoag, B. P.; Gin, D. L. *Macromolecules* **2000**, *33*, 8549.
(46) Lamparski, H.; O'Brien, D. F. *Macromolecules* **1995**, *28*, 1786.
(47) Unfortunately, it was not possible to accurately determine the extent of polymerization for LLC phases at elevated temperatures because our UV−Vis instrument does not have variable temperature capabilities.
(48) Odian, G. *Principles of Polymerization*, 3rd ed.; John Wiley & Sons: New York, 1991.

Table 2. Summary of Data for Molecules Polymerized in the L_α Phase[a]

compd	d_{100} before irradiation (Å)	d_{100} after irradiation (Å)	polymerized phase thermal stability (°C)
1d	31.4	31.9	> 300
1e	29.2	30.3	> 300
1f	31.2	31.8	N/A
1g	44.1	45.3	> 175
1h	34.5	39.7	> 300
1i	33.1	38.9	> 300

[a] Extent of conversion data via UV−vis are unavailable for compounds in the L_α phase because they do not exist at room temperature.

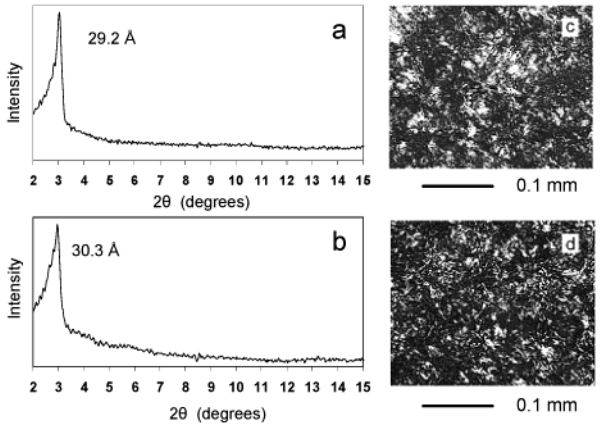

Figure 8. Representative XRD profiles and optical textures of the L_α phases of the gemini monomers before and after photopolymerization: (a) XRD pattern of **1e** (90 wt % in water, 62 °C) before photopolymerization; (b) XRD pattern of **1e** (90 wt % in water, 24 °C) after photopolymerization; (c) PLM micrograph of **1e** (90 wt % in water, 50 °C) before photopolymerization; and (d) PLM micrograph of **1e** (90 wt % in water, 24 °C) after photopolymerization.

tional monomer double bonds, [B] is the concentration of cross-linker double bonds, and X_w is the weight average degree of polymerization.[48] In our case, there is no monofunctional monomer present so [A] = 0, and the equation reduces to $\rho_c = 1/X_w$. Thus, to reach the gel point at 23% conversion, the weight average degree of polymerization only needs to be greater than five; and the higher the degree of polymerization, the less conversion is needed to cross-link the entire system.

Six molecules in the series (**1d**−**i**) exhibit an L_α phase, and the data from their polymerization in this phase are summarized in Table 2. Again, photopolymerization proceeded with retention of the phase, and representative before and after XRD and PLM profiles are shown in Figure 8. The PLM micrographs are essentially unchanged after irradiation, and the intensities of the observed XRD peaks are slightly reduced, similar to that in the H_I case. For the bilayer L_α phases, it appears that a general expansion of the unit cell occurs upon polymerization, which is unusual because cross-linking generally results in a small volume contraction.[48] These results were reproduced several times with different gemini homologues on a recalibrated XRD instrument, so this phenomenon is real and not due to XRD calibration error.[49] This expansion can be rationalized by loss of some tail interdigitation within the lamellar bilayers if the polymerization process causes the tail ends to shift up to join together. The fact that this apparent increase in *d* spacing upon polymerization is more pronounced in the gemini homologues with the longest tails (**1g**−**i**, $x = 14$) lends support to this

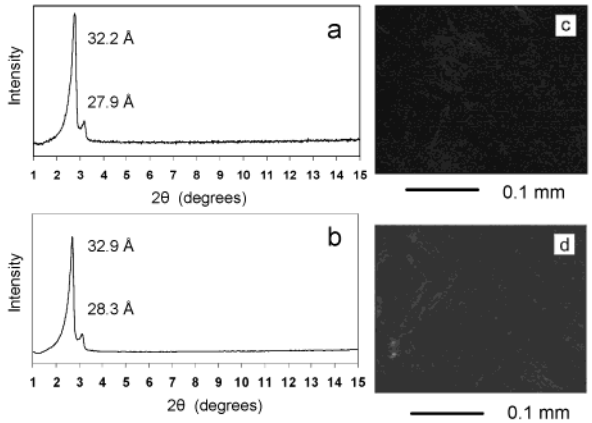

Figure 9. Representative XRD profiles and PLM optical textures of the Q_I phases of the gemini monomers before and after photopolymerization: (a) XRD pattern of **1e** (85 wt % in water, 35 °C) before photopolymerization; (b) XRD pattern of **1e** (85 wt % in water, 24 °C) after photopolymerization; (c) PLM micrograph of **1e** (85 wt % in water, 39 °C) before photopolymerization; and (d) PLM micrograph of **1e** (85 wt % in water, 24 °C) after photopolymerization.

supposition, since longer homologues would be expected to have a greater tendency for tail interdigitation.[50] A comparison of Tables 1 and 2 shows that this effect appears to be more pronounced in bilayer type assemblies (e.g., the L_α and Q phases) than in "monolayer" H phases in which there is more interfacial curvature. With respect to the stability of the cross-linked L_α phases, the thermal behavior of the irradiated phases is greatly improved over the nonirradiated phases. The optical textures of the polymerized samples are generally stable to greater than 300 °C. In the unpolymerized samples, water begins to boil off around 100 °C. Accurate extent of conversion information is unavailable for the L_α phases because these phases are only accessible at elevated temperatures.

Only four of the nine homologues (**1d**, **1e**, **1f**, and **1i**) form Q_I phases but each of these Q_I phases can be photocross-linked with retention of phase architecture. Representative XRD patterns and PLM micrographs taken before and after polymerization of these Q_I assemblies are presented in Figure 9. Table 3 summarizes the data from the polymerization runs of the three gemini monomers that form the more well-defined Q_I phases that appear between the H_I and L_α phases. The PLM optical textures remain essentially unchanged after polymerization. However, in this case complete loss of phase structure cannot be ruled out based on PLM data alone because the starting optical textures are pseudo-isotropic. The XRD patterns, however, confirm that the Q_I phases are intact after photopolymerization in each case, albeit with very slightly decreased peak intensities (Figure 9). Continuous long-term XRD analysis of some of the cross-linked Q_I phases (i.e., over 3−4 d) shows

(49) According to Bragg's law, *d* spacing (in Å) is inversely proportional to 2sin θ (in degrees). Consequently, small changes in 2θ result in progressively larger changes in *d* spacing at lower and lower angles, so the error in calculating d also gets progressively larger at lower 2θ angles. We are able to correct for a great deal of this error in the 1.5−3 degree range by using silver behenate (Kodak) as a low-angle diffraction standard (d_{100} = 58 Å) and collecting the XRD data as a high-resolution data file, so that the accuracy is within 1 Å in *d* spacing.

(50) Unfortunately, the degree of tail interdigitation cannot be determined experimentally from the XRD data. Although d_{100} directly gives the bilayer repeat distance, the bilayer spacing is the sum of an aqueous layer and the hydrocarbon tail segment. The thickness of these two components cannot be measured independently, so it is not possible to compare the actual hydrocarbon layer distance against the calculated extended length of the surfactants.

Table 3. Summary of Data for Three Gemini Monomers Polymerized in the Q_I Phase[a]

compd	d_{211} before irradiation (Å)	d_{211} after irradiation (Å)	polymerized phase thermal stability (°C)	extent of conversion (%)
1e	32.2	32.9	> 300	50
1h	34.1	40.4	> 300	N/A
1i	37.0	39.1	> 300	N/A

[a] Extent of conversion data via UV−vis are unavailable for compounds **1h** and **1i** in the Q_I phase because they do not exist at room temperature.

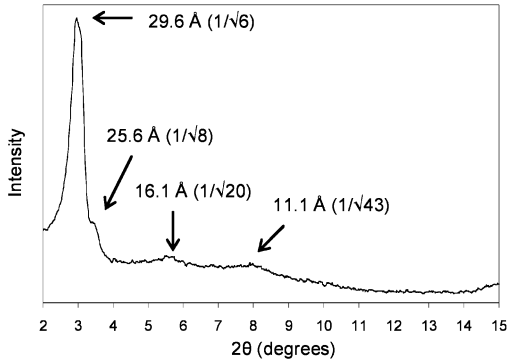

Figure 10. XRD profile of a cross-linked Q_I phase of **1e** showing higher order diffraction peaks (collected over a continuous scanning period of 84 h). Reflection d_{hkl} for a cubic phase has the relationship $m^2 = h^2 + k^2 + l^2$, such that d_{hkl} peak position is assigned a value of $(1/\sqrt{m})$ in terms of d spacing ratio.[40] The $1/\sqrt{20}$ peak is often observed in Q phases.[17,35,36] The smallest observed XRD peak at 11.1 Å matches with a cubic symmetry-allowed $1/\sqrt{43}$ peak, where h, k, l can be of the values 3, 5, and 3. (The d-values for this polymerized Q_I sample are slightly different from those presented in Figure 9 because this sample was prepared with slightly different water content.)

the presence of additional (albeit weak) higher-order d spacings (Figure 10) that definitively confirm a Q phase with *P* or *I* space group symmetry. As can be seen in Table 3, the Q_I phase unit cells expand upon cross-linking for the mesogens with the longest tail lengths (e.g., **1h**, **1i**), similar to that observed for the L_α phases. Again, this expansion upon cross-linking can be rationalized by loss of some tail interdigitation within the Q bilayers upon joining of the tail ends, and is more pronounced for the longer tail surfactants. The extent of 1,3-diene polymerization in the room-temperature Q_I phase of **1e** was found to be ca. 50% by UV−vis spectroscopy, again well above the expected gel point for these systems. All the resulting cross-linked Q_I assemblies possess good mechanical integrity and can be isolated as brittle solids or free-standing films that are insoluble in water and conventional organic solvents. These cross-linked LLC phases are also stable to at least 300 °C in air, as determined by variable temperature PLM (and supported by XRD).

We are currently exploring the use of these cross-linked H_I arrays are templates for forming anisotropic hybrid nanocomposites. With respect to the cross-linked Q_I systems, we are exploring methods for fabricating thin films of these nanoporous materials onto supports in order to examine their potential as novel membrane media for gas and liquid nanofiltration. Future work will focus on derivatizing the ionic headgroups in these assemblies with reactive moieties for new heterogeneous catalysis applications.

Conclusions

The synthesis and LLC phase behavior of a series of intrinsically cross-linkable gemini LLCs has been described. These novel polymerizable amphiphiles exhibit H_I, Q_I, and L_α phases in water and can be intrinsically photocross-linked with retention of phase architecture in each case. The Q_I phases formed by the reactive amphiphiles in this series have *P* or *I* space group symmetry from XRD analysis, and are most likely either a Q^{230} (*Ia*3*d*), a Q^{224} (*Pn*3*m*), a Q^{229} (*Im*3*m*), or a Q^{212} ($P4_32$) phase of Type I configuration, as inferred from their locations on the phase diagram and the physical properties of the cross-linked materials. The most likely candidate appears to be a Type I Q^{230} (*Ia*3*d*) phase, based on the aforementioned data and the phase behavior of monomeric amphiphiles of similar structure. The extent of conversion achieved in the LLC phases was determined by UV−vis spectrometry and found to be more than sufficient to extensively cross-link and stabilize the systems. The resulting cross-linked H_I, L_α, and Q_I assemblies exhibit excellent thermal robustness in air.

Acknowledgment. This research was supported in part by grants from the National Science Foundation (DMR-9642533), and the Office of Naval Research (N00014-00-1-0271 and N00014-02-1-0383). B.A.P. thanks Eli Lilly for a graduate fellowship during the initial part of this work. D.L.G. thanks the Alfred P. Sloan Foundation for a Research Fellowship. We also thank Prof. J. Arnold for use of his UV-vis spectrophotometers; J. Mellott and Prof. D. Schwartz for preliminary AFM studies; and Prof. E. Y.-X. Chen for his assistance in the TEM imaging studies.

Supporting Information Available: Detailed experimental procedures for the synthesis, characterization, LLC phase formation, and polymerization of the gemini monomers. A complete listing of the compositions, temperatures, and XRD data for the LLC phases identified in plotting the phase diagrams of the polymerizable gemini surfactants. Preliminary 2-D XRD and TEM images of the cross-linked Q_I phase of **1e**. Schematic representations of the six Q phase architectures observed so far for small molecule amphiphiles (PDF). This material is available free of charge via the Internet at http://pubs.acs.org.

JA0208106